

Assessing Structural Health State by Monitoring Peridynamics Parameters in Operational Conditions

Original

Assessing Structural Health State by Monitoring Peridynamics Parameters in Operational Conditions / Miraglia, Gaetano; Lenticchia, Erica; Civera, Marco; Ceravolo, Rosario. - 224:(2022), pp. 39-50. (Intervento presentato al convegno International Conference on Experimental Vibration Analysis for Civil Engineering Structures (EVACES)) [10.1007/978-3-030-93236-7_5].

Availability:

This version is available at: 11583/2971963 since: 2022-10-05T17:47:25Z

Publisher:

Springer

Published

DOI:10.1007/978-3-030-93236-7_5

Terms of use:

This article is made available under terms and conditions as specified in the corresponding bibliographic description in the repository

Publisher copyright

Springer postprint/Author's Accepted Manuscript

This version of the article has been accepted for publication, after peer review (when applicable) and is subject to Springer Nature's AM terms of use, but is not the Version of Record and does not reflect post-acceptance improvements, or any corrections. The Version of Record is available online at: http://dx.doi.org/10.1007/978-3-030-93236-7_5

(Article begins on next page)

Assessing Structural Health State by Monitoring Peridynamics Parameters in Operational Conditions

Gaetano Miraglia¹, Erica Lenticchia², Marco Civera³, Rosario Ceravolo⁴

¹ Ph.D., Department of Structural, Geotechnical and Building Engineering, Polytechnic of Turin - Turin, Italy.

² Ph.D., Department of Structural, Geotechnical and Building Engineering, Polytechnic of Turin - Turin, Italy.

³ Ph.D. Student, Department of Mechanical and Aerospace Engineering, Polytechnic of Turin - Turin, Italy.

⁴ Full Professor, Department of Structural, Geotechnical and Building Engineering, Polytechnic of Turin - Turin, Italy.

ABSTRACT

This paper aims to analyze the Peridynamics (PDs) theory and to exploit it for new possibilities in Civil Engineering by employing the theory for Structural Health Monitoring (SHM). In particular, the paper aims to exploit PDs for SHM and damage characterization of the built environment, at the structural scale, in operational conditions (i.e., without input sources). The reasons behind this study rely on the possibility to use PDs to emulate very complex structural behaviors effortlessly, using PDs as a paradigm to build low fidelity structural models of real systems. In the present paper, new features to characterize the damage (i.e., to detect, locate, and quantify it) are proposed thanks to a special definition of the peridynamic theory written in discrete form. These features are the Bond Extremity Acceleration (BEA) and Bond Extremity Velocity (BEV) conjectures, which are obtained by discretizing a system with the Bond Based PDs and using a micro-viscoelastic constitutive law at the bond level. Moreover, the authors show how the proposed peridynamic parameters are theoretically estimable with very robust techniques already used in SHM, such as the Stochastic Subspace Identification (SSI) algorithms. The considerations reported in the paper are verified with numerical (virtual) models. The paper concludes that PDs can be used to easily parametrize the built environment opening new research possibilities on the use of PDs for civil SHM. Additionally, the proposed BEA proves to be a very scalable and general parameter to be monitored in real systems (providing information on the presence, the location, and the amount of damage), this also due to its physical based meaning and the straightforward method of extraction in operational conditions.

Keywords: Peridynamics, Structural Health Monitoring, Damage Detection and Localization, Low Fidelity Structural Models, Structural Simulator.

1. INTRODUCTION

Finding the right balance between accuracy and computational efficiency of structural simulators is essential to obtain valuable information on the health state of real structures in a feasible computational time. In reaching this balance, the parallel use of low fidelity and high fidelity structural models is helpful, being the first approach ideal to extract very fast information, while the second able to generate high quality knowledge on complex behaviors of real systems. However, if Structural Health Monitoring (SHM) techniques need to be applied to a large number of structures (e.g., urban area), very high-fidelity models result to be inadequate to obtain information in a feasible computational time.

Peridynamics (PDs) is a modern nonlocal theory of continuum established in early 2000 by Stewart Silling [1], [2] and Silling et al. [3]. The theory is recently attracting attention in the field of computational mechanics since it replaces the partial differential equations of the classical continuum theory with integral, spatial equations. This allows overcoming problems related to the representation of discontinuities in the matter, which can arise during damage (e.g., cracks), where the differential formulations are not defined. A comprehensive literature review of Peridynamic (from the Greek words *peri-* i.e., around, and *-dynami* i.e. force) applications and uses can be found in [4]. Basically, PD theory found its principle in the forces-interaction (*bonds*) of points. The matter is divided into infinitesimal portions characterized by their mass and volume. Each point k is then supposed to interact with its neighbours inside a region. The collection of all the points inside this region is called *family* of k . The family of k is, in turn, characterized by the *horizon*, i.e., the maximum distance for which the interactions between k and the other points of a body occur. The horizon defines the locality of the behavior of a system; the smaller the horizon, the more local the behavior will be. It has been demonstrated that the classical theory of elasticity can be considered as a limiting case of the PD theory as the horizon approaches zero [5], [6], [7]. When using PD in a modelling phase, the choice of the horizon represents a crucial aspect. It can be a constant or variable along the modelling space. Sometime, physics defines the value of horizon (e.g., when modelling particles, the interatomic potential defines the maximum interaction distance). In other cases the

value of the horizon is not defined, and its definition should be based on calibration procedures [8]. When the standard local theory, instead, well describes the structural behavior, PD can still be used. In this case, the horizon should be as small as possible to fit the classical continuum theory, while when the nonlocal theory is used to model damage (e.g., crack growth and propagation), several works have related the value of the horizon with the value of the average distance between points used to discretize the continuum, [5], [8]. In this case, the horizon is commonly set to 3 times the spacing between points. PD is thus a candidate theory that can be used for modelling real systems. About the modelling of real systems, the work of Gosliga and Worden [9] is noteworthy. Here the authors propose the use of *Irreducible Element (IE) model*, which seeks to create a graphical representation of a system (using graph theory [10], [11], [12]) by breaking it down into its constituent parts, with the aim to assess the similarity of structures. The system modelling plays an important role in the SHM of existing systems [13], [14]. In this field, important researches have been done by Farrar and Worden et al. [15], [16], [17], while the promising future of this discipline is also dictated by the technological advancement of the last years [18]. The importance of system identification in SHM is crucial and is due to the advantage of using the information extracted from identification techniques for defining damage [19]. Within this framework, damage can be defined as a change introduced in a system that negatively affects its current and future performance [17]. Thus, SHM techniques are precisely intended to provide some physical/non-physical based damage index with a broad range of validity, in the linear and nonlinear field.

In the present paper the authors propose PDs as a general method to build physical-based graph representations (i.e., with edges and nodes) of civil structural systems (i.e., low fidelity models) and built environment. Then, starting from this representation, two features are proposed for an efficient damage identification and SHM: the Bond Extremity Acceleration (BEA) and Bond Extremity Velocity (BEV). This is done presenting the basic theory of PDs and the proposed algorithm to estimate the BEA and BEV (Section 2). Then, some numerical verifications supporting the theory is reported (Section 3). Finally, the conclusions are drawn (Section 4).

2. METHODS

In this section the methods are presented introducing the basic theory of Peridynamics and the procedure to identify the BEAs and BEVs using the Stochastic Subspace Identification (SSI) algorithms.

2.1. Basic theory

The linearized micro-linear viscoelastic Bond Based PD (BBPD) equation of motion can be written in standard form as (bold is herein used for vectors, bold capital for matrices and italic for scalars):

$$\mathbf{M}\ddot{\mathbf{u}}(t) + \mathbf{C}\dot{\mathbf{u}}(t) + \mathbf{K}\mathbf{u}(t) = \mathbf{z}(t)$$

$$\mathbf{M} = \begin{bmatrix} \mathbf{M}_k & \mathbf{0}_3 & \dots \\ \mathbf{0}_3 & \ddots & \dots \\ \vdots & \vdots & \ddots \end{bmatrix}; \mathbf{C} = \begin{bmatrix} \sum_{j=1, j \neq k}^K \mathbf{C}_{kj} & -\mathbf{C}_{kj} & \dots \\ & \ddots & \dots \\ -\mathbf{C}_{kj} & \ddots & \dots \\ \vdots & \vdots & \ddots \end{bmatrix}; \mathbf{K} = \begin{bmatrix} \sum_{j=1, j \neq k}^K \mathbf{K}_{kj} & -\mathbf{K}_{kj} & \dots \\ & \ddots & \dots \\ -\mathbf{K}_{kj} & \ddots & \dots \\ \vdots & \vdots & \ddots \end{bmatrix} \quad (1)$$

where:

$$\begin{aligned} \mathbf{M}_k &= m_k \mathbf{I}_3 \\ \mathbf{C}_{kj} &= v_{kj} \mathbf{K}_{kj} \\ \mathbf{K}_{kj} &= c_{kj} V_j V_k \mathbf{\Xi}_{kj} \\ \mathbf{\Xi}_{kj} &= \frac{\boldsymbol{\xi}_{kj} (\boldsymbol{\xi}_{kj}^T)}{\|\boldsymbol{\xi}_{kj}\|^3} \\ c_{kj} &= \begin{cases} c_{kj} & \text{if } \|\boldsymbol{\xi}_{kj}\| \leq h \\ 0 & \text{if } \|\boldsymbol{\xi}_{kj}\| > h \end{cases} \\ \boldsymbol{\xi}_{kj} &= \mathbf{x}_j - \mathbf{x}_k \end{aligned} \quad (2)$$

In Eq. (1) and Eq. (2) $\mathbf{x}_k = (x_{k,X}, x_{k,Y}, x_{k,Z})^T$ are the coordinates X, Y, Z of point k (similarly for j), $c_{kj} \geq 0$ is called bond elastic constant, and h is the horizon. V_j and V_k are the volumes associated to the points j and k respectively while $v_{kj} \geq 0$ is a bond damping constant; m_k is the mass associated to the point k , \mathbf{I}_3 is a 3x3 identity matrix and \mathbf{O}_3 is a 3x3 zero matrix. K is the number of points used to discretize the system. Then, $\mathbf{u}(t)$ and $\mathbf{z}(t)$ denote the displacement vector and the external force vector respectively, being t the time variable and $(\dots)(t)$ the time derivate operator. Finally, \mathbf{M} , \mathbf{C} , and \mathbf{K} denote the mass, damping, and stiffness global matrices of the system.

2.2. Parameters identification

From Eq. (1) and Eq. (2) it is possible to derive two parameters that can be easily experimentally identified without input (operational conditions) sources; the Bond Extremity Acceleration (BEA) w'_{kj} , and the Bond Extremity Velocity (BEV) w''_{kj} , of the bond kj and the extremity k , which are here proposed as parameters to be monitored for SHM purpose:

$$\begin{aligned} w'_{kj} &= \frac{c_{kj} V_j V_k}{m_k} \\ w''_{kj} &= w'_{kj} v_{kj} \end{aligned} \quad (3)$$

It is worth noting that in Eq. (3), in general, $w'_{kj} \neq w'_{jk}$ and $w''_{kj} \neq w''_{jk}$ as $m_k \neq m_j$.

Starting from the acquired acceleration response $\ddot{\mathbf{u}}(t)$ it is possible to get an estimate of the system matrix $\hat{\mathbf{A}}$ (in the state space formulation) reduced to the number of recorded Degree of Freedoms (DoFs), by using, for instance, SSI algorithms. The eigenanalysis performed on $\hat{\mathbf{A}}$ provide its eigenvalues $\mathbf{\Lambda}$, eigenvectors $\mathbf{\Phi}$, and modal damping ratios \mathbf{Z} , where $\mathbf{\Lambda}$ is a diagonal matrix containing the sorted eigenvalues on the main diagonal, \mathbf{Z} is a diagonal matrix containing the corresponding damping ratios on the main diagonal, while $\mathbf{\Phi}$ is the eigenvectors matrix containing the corresponding eigenvectors in each column of the matrix. Performing the estimate of $\hat{\mathbf{A}}$ on a dimension equal to the number of recorded DoFs, it is possible to get an estimate of the mass $\hat{\mathbf{M}}$, damping $\hat{\mathbf{C}}$, and stiffness $\hat{\mathbf{K}}$ global matrices of the system reduced to these DoFs:

$$\begin{aligned} \hat{\mathbf{K}} &= (\mathbf{\Phi}^T)^{-1} (\mathbf{\Lambda}) (\mathbf{\Phi})^{-1} \\ \hat{\mathbf{M}} &= (\mathbf{\Phi}^T)^{-1} (\mathbf{I}) (\mathbf{\Phi})^{-1} \\ \hat{\mathbf{C}} &= (\mathbf{\Phi}^T)^{-1} (2\mathbf{Z}\sqrt{\mathbf{\Lambda}}) (\mathbf{\Phi})^{-1} \end{aligned} \quad (4)$$

where \mathbf{I} is an identity matrix with the same dimension of $\mathbf{\Lambda}$. Then, the BEAs and the BEVs can be estimated with:

$$\begin{aligned} \hat{\mathbf{W}}' &= \left[-(\hat{\mathbf{M}})^{-1} (\hat{\mathbf{K}}) \right] (\mathbf{\Delta})^{\circ-1} \\ \hat{\mathbf{W}}'' &= \left[-(\hat{\mathbf{M}})^{-1} (\hat{\mathbf{C}}) \right] (\mathbf{\Delta})^{\circ-1} \\ \mathbf{\Delta} &= \begin{bmatrix} \mathbf{I}_3 & \mathbf{\Xi}_{kj} & \dots \\ \mathbf{\Xi}_{kj} & \ddots & \dots \\ \vdots & \vdots & \ddots \end{bmatrix} \end{aligned} \quad (5)$$

where $(\dots)^{\circ-1}$ denotes the Hadamard inversion operator, while $\hat{\mathbf{W}}'$ and $\hat{\mathbf{W}}''$ contain the estimate of the BEAs w'_{kj} , and the BEVs w''_{kj} , respectively. The estimates of these features can be then refined by repeating the identification procedure on a second estimate of the of the system matrix $\hat{\hat{\mathbf{A}}}$:

$$\hat{\hat{\mathbf{A}}} = \begin{bmatrix} \mathbf{O} & \mathbf{I} \\ -(\hat{\mathbf{M}})^{-1} (\hat{\mathbf{K}}) & -(\hat{\mathbf{M}})^{-1} (\hat{\mathbf{C}}) \end{bmatrix} \quad (6)$$

obtaining the refined estimate of BEAs $\hat{\hat{\mathbf{W}}}'$, and BEVs $\hat{\hat{\mathbf{W}}}''$.

3. RESULTS AND DISCUSSION

In this section the previous described methods are applied to numerical benchmarks, and the verifications of the study are reported and discussed.

The numerical benchmarks are represented by 2 Multi Degree of Freedoms (MDoFs) systems. The first with 4 DoFs, while the second with 10 DoFs. For the sake of clarity, the systems are represented by a series of masses (spaced 1 m from each other) which vibrate in one direction. The systems are supposed to do not have a unique value of the masses or volumes, but these values are randomly extracted between 0.8 and 1 (for both mass [kg] and volume [m³] values). Thus, for the 4 DoFs system, 100 extractions of the model parameters (masses and volumes) have been performed. The same has been done for the 10 DoFs system. A dummy mass has been added to the systems in order to constrain the problem and avoid rigid body motions. Then, for each system, 4 cases of acquisitions have been assumed: 10 and 30 minutes of acquisitions with signals corrupted by a 5% and 20% of gaussian noise. The sampling frequency has been supposed equal to 100 Hz. The horizon h , has been set to 3 m, while $c_{kj} = 2e3 \text{ N/m}^6$, and $v_{kj} = 1e - 3 \text{ sec}$.

The methods described in Section 2 have been then applied and the discrepancy between *target* (theoretically correct) values and identified values of the BEAs and BEVs has been studied. Fig. 1 reports the Probability Density Function (PDF) of the *average identification error* (mean values over the bonds of the absolute difference between target and identified values of BEAs and BEVs, normalized to the target value). Each PDF has been estimated with 100 samples. From the figure is possible to conclude that the error of BEV is higher and more dispersed than the error of BEA, and the error tend to decrease as the signal length increase.

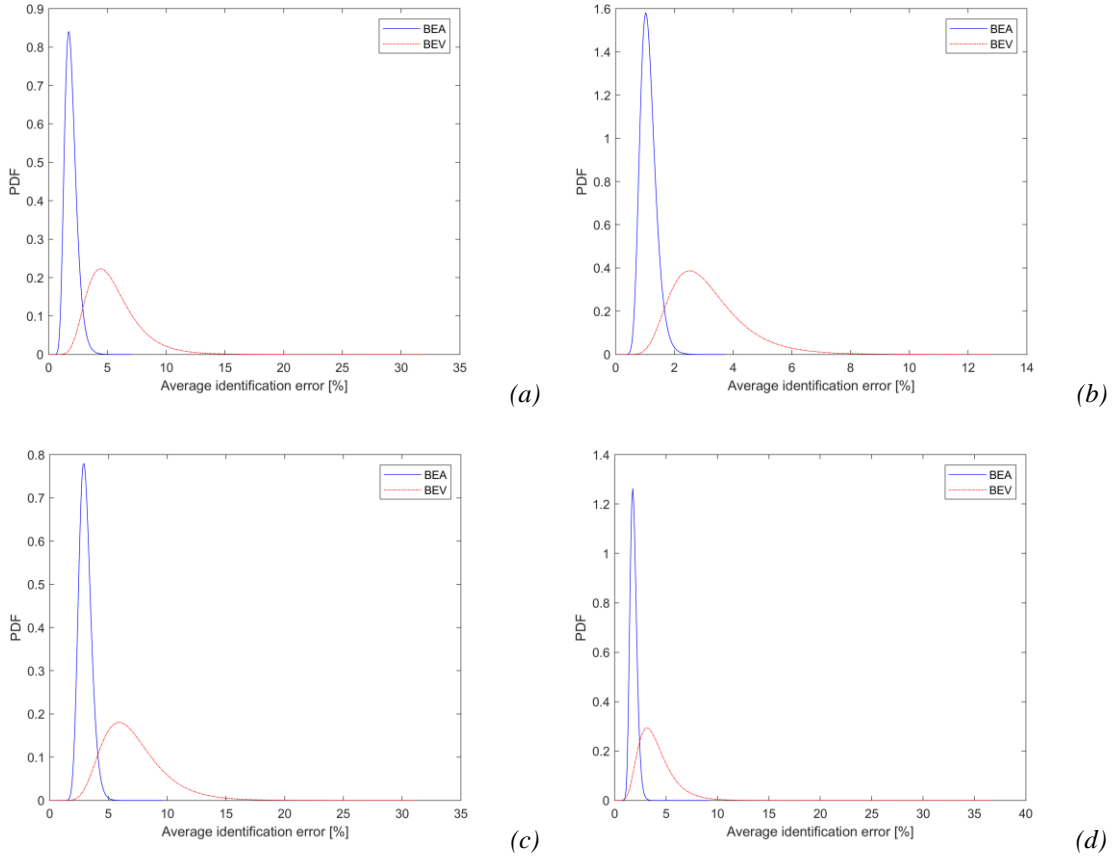
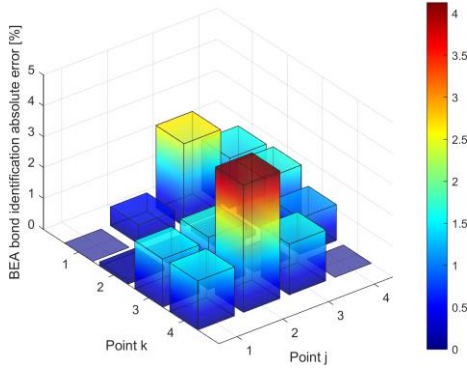
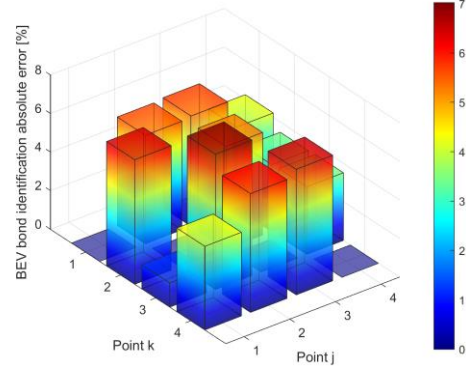


Fig. 1 Probability Density Function (PDF) of the average identification error [%] of BEAs and BEVs for a 4 DoFs system with 10 minutes (a), and 30 minutes (b) of records, and for a 10 DoFs system with 10 minutes (c) and 30 minutes (d) of records. All plots refer to 5% of gaussian noise in the records.

Fig. 2 depicts the *bond identification absolute error* (absolute difference between target and identified values of BEAs and BEVs, normalized to the target value, for each bond) for a case of the 4 DoFs system, with 10 minutes of records corrupted by 5% of gaussian noise. Also in this case it is possible to note as the errors on the bonds are higher for the estimates of the BEVs.



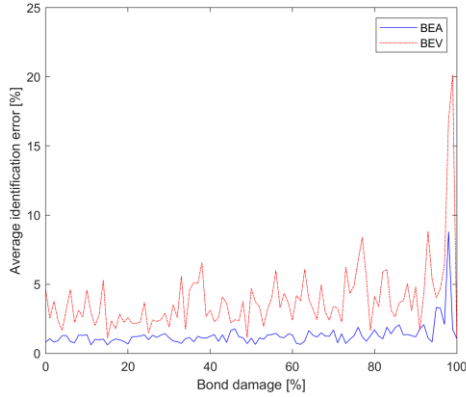
(a)



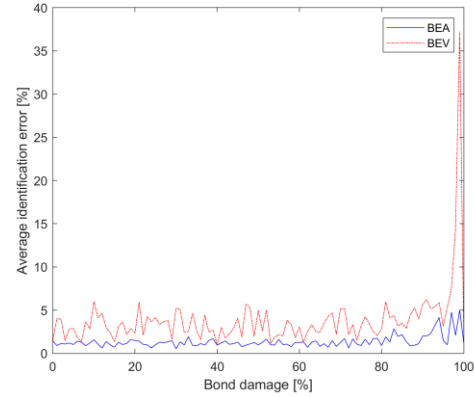
(b)

Fig. 2 Absolute identification errors [%] of BEAs (a) and BEVs (b) of the bonds k - j , for a generic 4 DoFs system with 10 minutes of records and 5% of gaussian noise in the records.

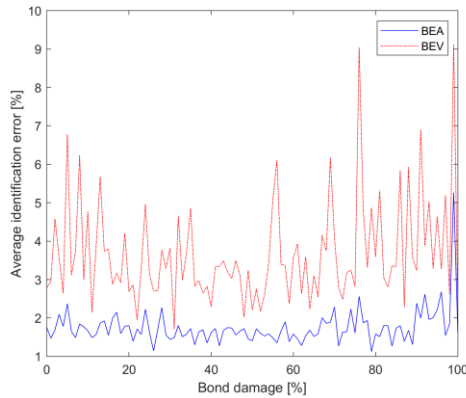
Then, a realization of the model parameters (masses and volumes) for the 4 DoFs and the 10 DoFs system has been used to study the *average identification error* at increasing damage. In this study, the first bond (bond between points 1 and 2) and the last bond (bond between points 3 and 4 for the 4 DoFs system, and between points 9 and 10 for the 10 DoFs system) have been damaged. It was supposed a damage multiplier (*bond damage*) between 0 and 1. This multiplier defines the new values of c_{12} and c_{21} as proportional to the initial value of $2e3 \text{ N/m}^6$. For the last bond it was assumed a damage multiplier equal to the half of that one used for the first bond. Fig. 3 reports the *average identification error* for some analyzed cases as a function of the *bond damage*.



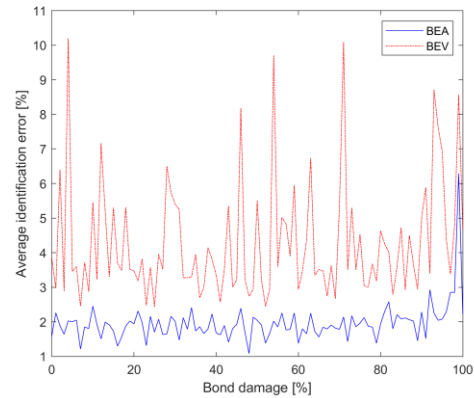
(a)



(b)



(c)



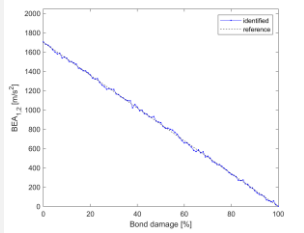
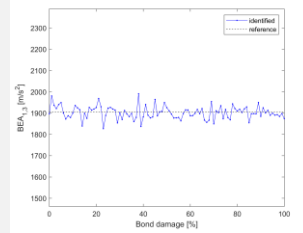
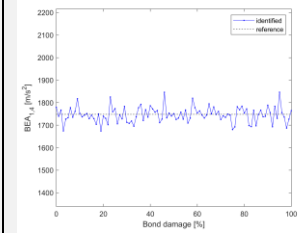
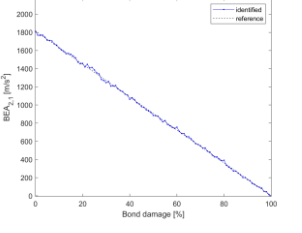
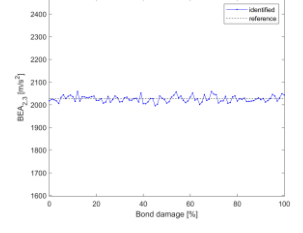
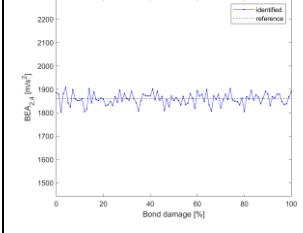
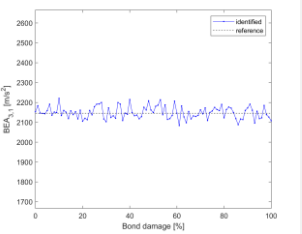
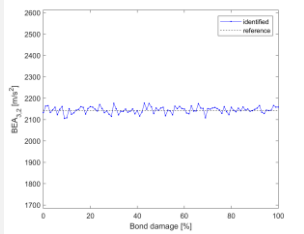
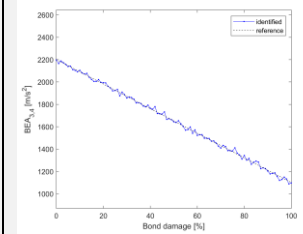
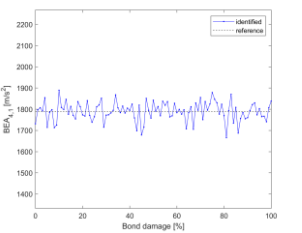
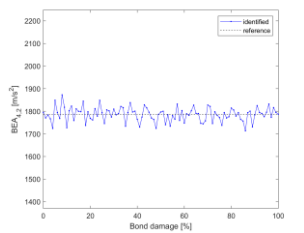
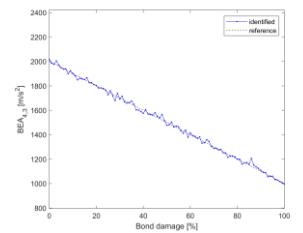
(d)

Fig. 3 Average identification error [%] of BEAs and BEVs as a function of the damage level [%] on the bond 1-2 for a 4 DoFs system with 5% (a), and 20% (b) of gaussian noise in the records, and for a 10 DoFs system with 5% (c), and 20% (d) of gaussian noise in the records. All plots refer to 30 minutes of records.

From Fig. 3 it is possible to conclude that the error remains quite stable at increasing percentage of noise in data, and generally is higher and more unstable for the estimate of the BEVs. Then, Table 1 reports the comparison between target and identified values of BEAs as a function of the *bond damage* for the 4 DoFs system.

From the table is easy to observe that the only damaged bonds are those expected to be damaged, and the amount of damage is consistence with the expected values. In fact, the first bond reaches a value of BEA equal to 0, while the last bond reach half of its initial value for a bond damage on the first bond equal to 100%. Finally, the BEA values of the remaining bonds rightly remain unchanged as the damage increases.

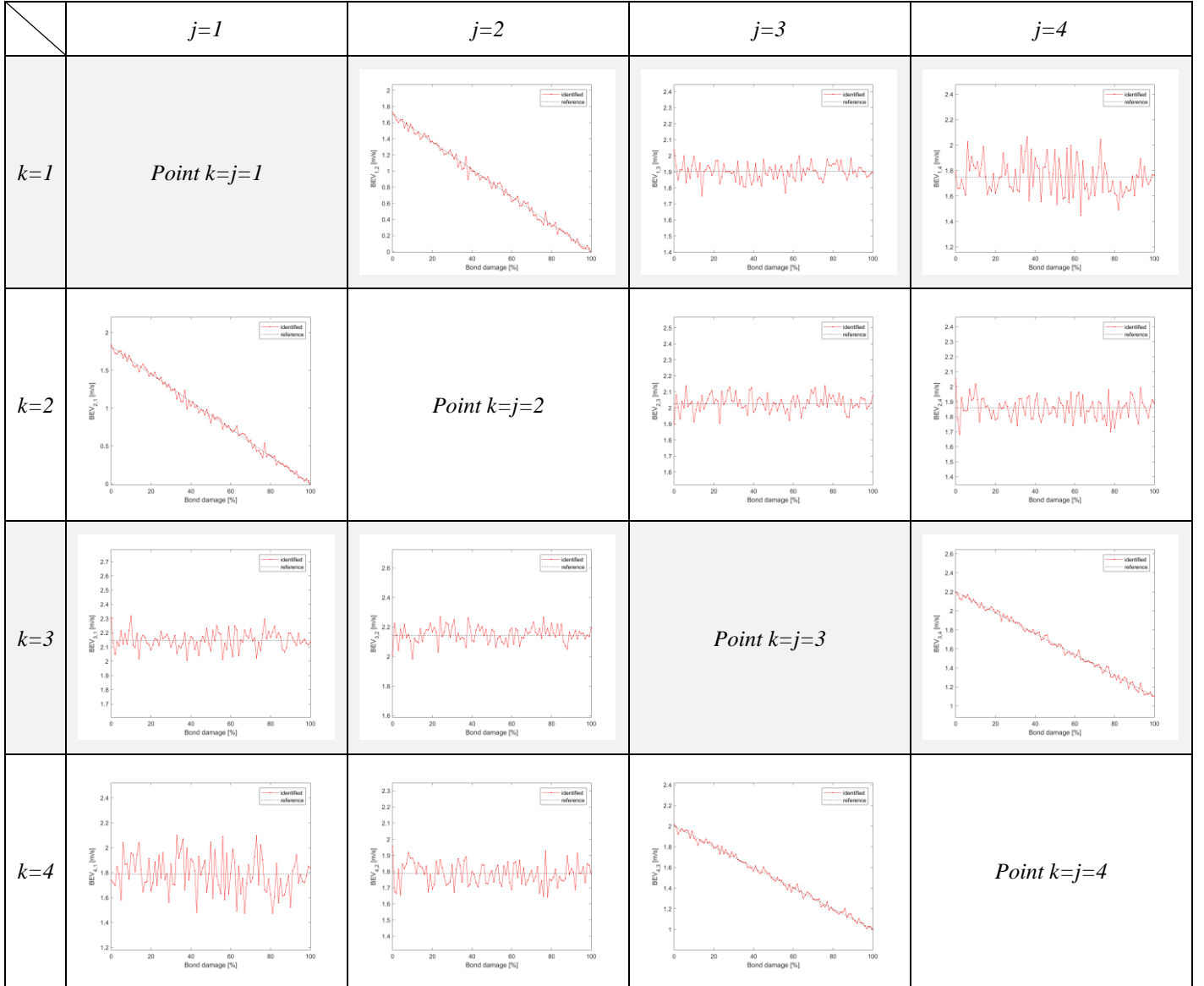
Table 1. Discrepancy between target (dashed black line) and identified BEAs [m/s^2] (blue line) as a function of the damage level [%] on the bond 1-2 for a 4 DoFs system with 30 minutes of records and 5% of gaussian noise in the records.

	$j=1$	$j=2$	$j=3$	$j=4$
$k=1$	<i>Point $k=j=1$</i>			
$k=2$		<i>Point $k=j=2$</i>		
$k=3$			<i>Point $k=j=3$</i>	
$k=4$				<i>Point $k=j=4$</i>

Finally, as done for BEA, Table 2 reports the comparison between target and identified values of BEVs as a function of the *bond damage* for the 4 DoFs system.

From the table is easy to observe that the only damaged bonds are those expected to change value, and the amount of changing is consistence with the expected values. In fact, the first bond reaches a value of BEV equal to 0, while the last bond reach half of its initial value for a bond damage on the first bond equal to 100%. Finally, the BEV values of the remaining bonds rightly remain unchanged as the damage increases, even if compared to the BEAs estimates, the BEVs values fluctuate more around the target values.

Table 2. Discrepancy between target (dashed black line) and identified BEVs [m/s] (red line) as a function of the damage level [%] on the bond 1-2 for a 4 DoFs system with 30 minutes of records and 5% of gaussian noise in the records.



4. CONCLUSIONS

In the paper, the authors proposed Peridynamics as a generic method to generate low fidelity structural models and obtaining valuable and very fast information on the health state of a large number of structures. Then, the authors found that Peridynamics can be used to define physical-based graph representations (i.e., with edges and nodes) of civil structural systems. These findings, for now limited to numerical verifications, demonstrate that Peridynamics proves ideal for facing the SHM of vast territories with computational effortless strategies, and physical-based (i.e., providing valuable information) representations of the built environment. In this regard, the proposed BEA proves to be a very scalable and general parameter to be monitored in real systems (providing information on the presence, the location, and the amount of damage), this also due to its physical based meaning and the straightforward method of extraction in operational conditions. About the results of the numerical verifications, it is possible to draw the following conclusions:

- The identification errors for BEV are generally larger and more dispersed (greater uncertainty) than those for BEA.
- The estimate of BEA and BEV remain quite stable to an increase of the percentage of noise in the records, while the errors little increase if the length of the acquisitions decrease.
- The BEA can be used for the damage identification, i.e., to detect, quantify, and localize the damage.

- The BEV, instead, is a dubious parameter, since its use strongly depends by the discrepancy between the model and the actual behavior of the system; therefore, its use for SHM purposes should be carefully evaluated.

The authors envisage low fidelity peridynamic models as a general method to allow physical-based SHM of systems over a territorial scale. For example, our results can be useful to generate network of built structures helping in the early warning of catastrophic events such as earthquakes, hurricanes, tornadoes, landslides, etc. In addition, structures built in the first half of the twentieth century are approaching or have surpassed their typical design life, meaning that there is a need to check the state of aging of structures over large areas. In this regard, low fidelity peridynamic models can be used to monitor very slow or sudden changes of structural states relying on very robust algorithms from established literature.

Although the results of the numerical verifications are promising, all considerations made must pass the experimental validation phase to be considered valid, which can represent the next step of this work.

ACKNOWLEDGMENTS

None.

REFERENCES

- [1] S. A. Silling, "Reformulation of elasticity theory for discontinuities and long-range forces," *J. Mech. Phys. Solids*, vol. 48, no. 1, pp. 175–209, 2000.
- [2] S. A. Silling, "Peridynamic modeling of the Kalthoff--Winkler experiment," *Submiss. 2001 Sandia Prize Comput. Sci.*, 2001.
- [3] S. A. Silling, M. Epton, O. Weckner, J. Xu, and E. Askari, "Peridynamic states and constitutive modeling," *J. Elast.*, vol. 88, no. 2, pp. 151–184, 2007.
- [4] A. Javili, R. Morasata, E. Oterkus, and S. Oterkus, "Peridynamics review," *Math. Mech. Solids*, vol. 24, no. 11, pp. 3714–3739, 2019.
- [5] E. Madenci and E. Oterkus, *Peridynamic theory and its applications*, vol. 17. Springer, 2014.
- [6] S. A. Silling, M. Zimmermann, and R. Abeyaratne, "Deformation of a peridynamic bar," *J. Elast.*, vol. 73, no. 1–3, pp. 173–190, 2003.
- [7] O. Weckner and R. Abeyaratne, "The effect of long-range forces on the dynamics of a bar," *J. Mech. Phys. Solids*, vol. 53, no. 3, pp. 705–728, 2005.
- [8] F. Bobaru, J. T. Foster, P. H. Geubelle, and S. A. Silling, *Handbook of peridynamic modeling*. CRC press, 2016.
- [9] J. GOSLIGA and K. WORDEN, "A General Representation for Assessing the Similarity of Structures," *Struct. Heal. Monit.* 2019, 2019.
- [10] J. A. Bondy, U. S. R. Murty, and others, *Graph theory with applications*, vol. 290. Macmillan London, 1976.
- [11] D. B. West and others, *Introduction to graph theory*, vol. 2. Prentice hall Upper Saddle River, 2001.
- [12] D. J. Sanderson, D. C. P. Peacock, C. W. Nixon, and A. Rotevatn, "Graph theory and the analysis of fracture networks," *J. Struct. Geol.*, vol. 125, pp. 155–165, 2019.
- [13] H. Sohn *et al.*, "A review of structural health monitoring literature: 1996--2001," *Los Alamos Natl. Lab. USA*, pp. 1–7, 2003.
- [14] J. P. Amezcua-Sanchez and H. Adeli, "Nonlinear measurements for feature extraction in structural health monitoring," *Sci. Iran.*, vol. 26, no. 6, pp. 3051–3059, 2019.
- [15] T. J. Rogers, K. Worden, R. Fuentes, N. Dervilis, U. T. Tygesen, and E. J. Cross, "A Bayesian non-parametric clustering approach for semi-supervised Structural Health Monitoring," *Mech. Syst. Signal Process.*, vol. 119, pp. 100–119, 2019.
- [16] C. R. Farrar and K. Worden, "An introduction to structural health monitoring," *Philos. Trans. R. Soc. A Math. Phys. Eng. Sci.*, vol. 365, no. 1851, pp. 303–315, 2007.
- [17] C. R. Farrar and K. Worden, *Structural health monitoring: a machine learning perspective*. John Wiley & Sons, 2012.
- [18] S. Sony, S. Laventure, and A. Sadhu, "A literature review of next-generation smart sensing technology in structural health monitoring," *Struct. Control Heal. Monit.*, vol. 26, no. 3, p. e2321, 2019.
- [19] Z. Wang, R. M. Lin, and M. K. Lim, "Structural damage detection using measured FRF data," *Comput. Methods Appl. Mech. Eng.*, vol. 147, no. 1–2, pp. 187–197, 1997.